Surface & Coatings Technology 365 (2019) 152–157

Contents lists available at ScienceDirect

Surface & Coatings Technology

journal homepage: www.elsevier.com/locate/surfcoat

High-ion-energy and low-temperature deposition of diamond-like carbon (DLC) coatings with pulsed kV bias☆

Xiaokai An[a], Zhongzhen Wu[a,b,c,*], Liangliang Liu[a], Tielei Shao[a], Shu Xiao[a], Suihan Cui[a], Hai Lin[a], Ricky KY Fu[b], Xiubo Tian[a], Paul K Chu[b,c,**], Feng Pan[a,***]

[a] School of Advanced Materials, Peking University Shenzhen Graduate School, Shenzhen 518055, China
[b] Department of Physics, City University of Hong Kong, Tat Chee Avenue, Kowloon, Hong Kong, China
[c] Department of Materials Science and Engineering, City University of Hong Kong, Tat Chee Avenue, Kowloon, Hong Kong, China

ARTICLE INFO

Keywords:
DLC
Substrate bias
Adhesion
Mechanical properties
Electrochemical corrosion properties

ABSTRACT

The high ion energy produced by the substrate bias is essential to the enhancement of the sp^3 content in diamond-like carbon (DLC) coatings and adhesion with the substrate. However, excessive ion energy can turn into heat conversely converting sp^3 into sp^2 undermining the mechanical properties. In this work, pulsed kV bias is applied to increase the carbonous ion energy to increase the sp^3 content in DLC coatings and improve the adhesion with the substrate simultaneously while avoiding adverse temperature increase. The high ionized carbonous ions flux is formed by an anode-layer ion source with C_2H_2 gas and $Cr/CrC_x/CrC$ interlayers are introduced between the DLC coating and high-speed steel (HSS) substrate to release the internal stress by high-power impulse magnetron sputtering (HiPIMS). The DLC coatings not only have a large sp^3 content, high hardness of 18.5 GPa, a low friction coefficient of 0.12, superior anti-corrosion behaviors,and wear rate of 0.87×10^{-15} m^3/N m for 4 h, but also exhibits outstanding adhesion (Lc = 76 N) with the HSS substrate in spite of a DLC coating thickness of 13 μm.

1. Introduction

Diamond-like carbon (DLC) coating, a metastable form of amorphous carbon with mixed hybridizations of sp^2 and sp^3 [1,2], have excellent mechanical hardness, chemical inertness, tribological properties such as low friction and wear properties [3–5], as well as self-lubrication for hydrogenated coatings [6–8]. DLC coatings are widely used as protective coatings on cutting tools, biomedical devices, and microelectromechanical devices (MEMs) [1]. However, the high internal stress in the coatings leads to a poor adhesion with many substrates [9], especially for DLC coatings thicker than 3 μm. The internal stress in DLC coatings can be reduced but the hardness, self-lubrication, and corrosion resistance are sacrificed [10,11]. The ion energy produced by the substrate bias can improve the sp^3 content which need more energy to form than sp^2 [12] in DLC coatings and adhesion with the substrate, but an excessively large ion energy creates heat that converts sp^3 into sp^2 thus worsening the mechanical properties. In physical vapor deposition (PVD), the substrate bias is typically < 1 kV DC and in plasma immersion ion implantation & deposition (PIII&D), the pulsed substrate bias is always > 10 kV in order to perform ion implantation [2–4]. When a DC bias is applied, the hardness and adhesion increase initially with increasing bias by producing more sp^3 hybridization and strengthening the interface. However, the too large bias leads to ion-beam-induced thermal effects, converting sp^3 to sp^2 and undermining the mechanical properties. While, although the bias is pulsed, the high voltage of PIII&D (> 10 kV) is too large for DLC deposition, and in fact, the mechanical properties decrease monotonically with substrate bias [13–16].

In this study, in order to avoid excessive heating while increasing the carbonous ions energy to improve the sp^3 fraction [16–18] and film adhesion, a medial pulsed bias (1–10 kV) with a low duty cycle of 0.5% is adopted to prepare DLC coatings. The effects of the substrate bias on the structure, mechanical properties and electrochemical performances of the DLC coatings are studied systematically. The 13 μm thick coating has a high hardness of 18.5 GPa, superior anti-corrosion behaviors, as well as excellent tribological characteristics such as a small friction

☆ The 14th International Conference on Plasma Based Ion Implantation & Deposition(PBII&D 2017) ID: 101

* Correspondence to: Z.Z. Wu, School of Advanced Materials, Peking University Shenzhen Graduate School, Shenzhen 518055, China.
** Correspondence to: P.K. Chu, Department of Physics, City University of Hong Kong, Tat Chee Avenue, Kowloon, Hong Kong, China.
*** Corresponding author.
E-mail addresses: wuzz@pkusz.edu.cn (Z. Wu), paul.chu@cityu.edu.hk (P.K. Chu), Panfeng@pkusz.edu.cn (F. Pan).

https://doi.org/10.1016/j.surfcoat.2018.08.099
Received 29 March 2018; Received in revised form 15 August 2018; Accepted 31 August 2018
Available online 30 September 2018
0257-8972/

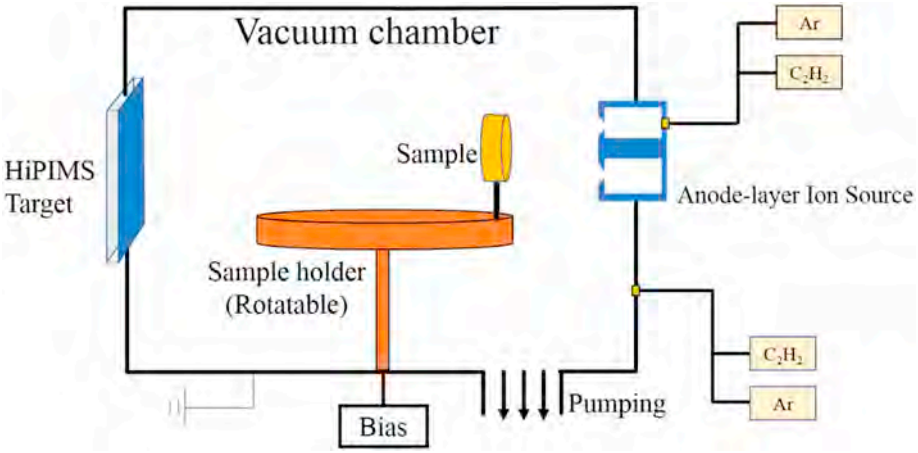

Fig. 1. Schematic diagram of homemade multifunctional plasma surface modification and deposition system and substrates' position.

coefficient of 0.12, low wear rate of 0.87×10^{-15} m^3/N·m for 4 h, and excellent adhesion of 76 N.

2. Experimental details

The homemade multifunctional plasma surface modification and deposition system with a diameter of 100 cm and height of 80 cm is shown in Fig. 1. The base pressure was 8×10^{-4} Pa. The substrates for the hydrogenated amorphous carbon (a:C—H) films were mirror-polished silicon (100), high-speed steel (HSS,Φ25 × 4 mm) and stainless steel (SS, 4 × 3 cm) and were set at 15 cm from target or anode-layer ion source. Before deposition, they are ultrasonically cleaned in alcohol, acetone, and deionized water for 30 min each. An anode-layer ion source was operated at 800 V and 0.45 A to produce the Ar plasma to perform pre-cleaning for 20 min (40 sccm, 99.999% purity) at 0.8 Pa and DC bias of −800 V. The Cr/CrCx/CrC interlayer [13] was deposited by HiPIMS using a Cr target (99.9% at.%) and a gradient atmosphere of Ar and C_2H_2 at a DC bias between 800 V and 100 V and a pressure of 0.8 Pa, as shown in Table 1. The HiPIMS voltage is 750 V, 50 Hz, 300 μs with about 320 A of peak current. Cr layer was deposited in pure Ar (30 sccm) atmosphere firstly by HiPIMS with 800 V DC bias in 2 min. Then C_2H_2 was added into vacuum chamber with a flow from 0 sccm to 30 sccm and DC bias decreased from 800 V to 100 V in 8 min. Finally, 30 sccm C_2H_2 and 100 V bias were used to deposit C rich CrC layer for 2 min. The C plasma was produced by anode-layer ion source to deposit DLC coatings in Ar and C_2H_2 [10/45 sccm, C_2H_2 (99.8% purity)] atmosphere [19–21]. To evaluate the effects of the pulsed bias, 1.5 kV, 3.5 kV, 5.5 kV, 7.5 kV, and 9.5 kV were and the frequency and width of the pulsed bias were kept at 50 Hz and 100 μs.

Field-emission scanning electron microscopy (FE-SEM, ZEISS SUPRA® 55) and energy-dispersive X-ray spectrometry (EDS) were employed to determine the microstructure, thickness, and composition of the coatings. The bonding information was obtained by high-resolution confocal Raman scattering (Horiba LAabRam HR VIS) with a 532 nm laser as the excitation source and X-ray photoelectron spectroscopy (ESCALAB 250×, Thermo Fisher, England) with a pass energy of 20 eV and an analysis time of 50 ms. The nanoindentor (Hysitron TI 950) in the Nano Dynamic Mechanical Analysis mode was used to measure the micro-hardness and each sample was tested five times at different locations to improve the accuracy. The adhesion strength between the coatings and substrates was measured on a scratch tester (WS - 2005, Zhongke Kaihua Technology, China) equipped with acoustic emission and the scratch patterns were captured by a 3D laser scanning microscope (KEYENCE, VK - X200). The load was gradually increased from 0 N to 100 N at rates of 3 mm/min and 50 N/min. The friction coefficients and wear resistance were determined on a ball-on disk tester (Rtec MFT - 5000) at a relative humidity of 65 ± 1% and temperature of 25 ± 1 °C. A Si_3N_4 ball (Φ3 mm) was used against the coatings at 4 N and 200 rpm and the wear radius was 5 mm. Electrochemical corrosion properties of DLC films and SS substrate were characterized with polarization curves, impedance modulus and phase-angle Bode diagrams by electrochemical workstation (CHI - 604E, Shanghai Chenhua). The three-electrode system consisted with a platinum stuck counter electrode, a working electrode (WE) and a saturated calomel reference electrode (SCE) and 3.5% NaCl solution were used as electrolyte in the Tafel model at room temperature. The sweeping range of polarization curves was - 1.5 to + 1 V and the contact area between electrolyte and sample was 1.77 cm^2.

3. Results and discussion

Fig. 2 shows the cross-sectional morphologies of the DLC coatings

Table 1
Experimental parameters in Cr/CrC_x/CrC interlayer and DLC coatings deposition.

		Ar (sccm)	C_2H_2 (sccm)	Bias (V)	Time (min)	Gas pressure(Pa)
Interlayer	Period I	30	0	−800	2	0.8
	Period II	30	0–30	−100	8	
	Period III	30	30	−100	2	
DLC coating		10	45	−1500 (50 Hz,100 μs)	840	0.5
		10	45	−3500 (50 Hz,100 μs)	840	
		10	45	−5500 (50 Hz,100 μs)	840	
		10	45	−7500 (50 Hz,100 μs)	840	
		10	45	−9500 (50 Hz,100 μs)	840	

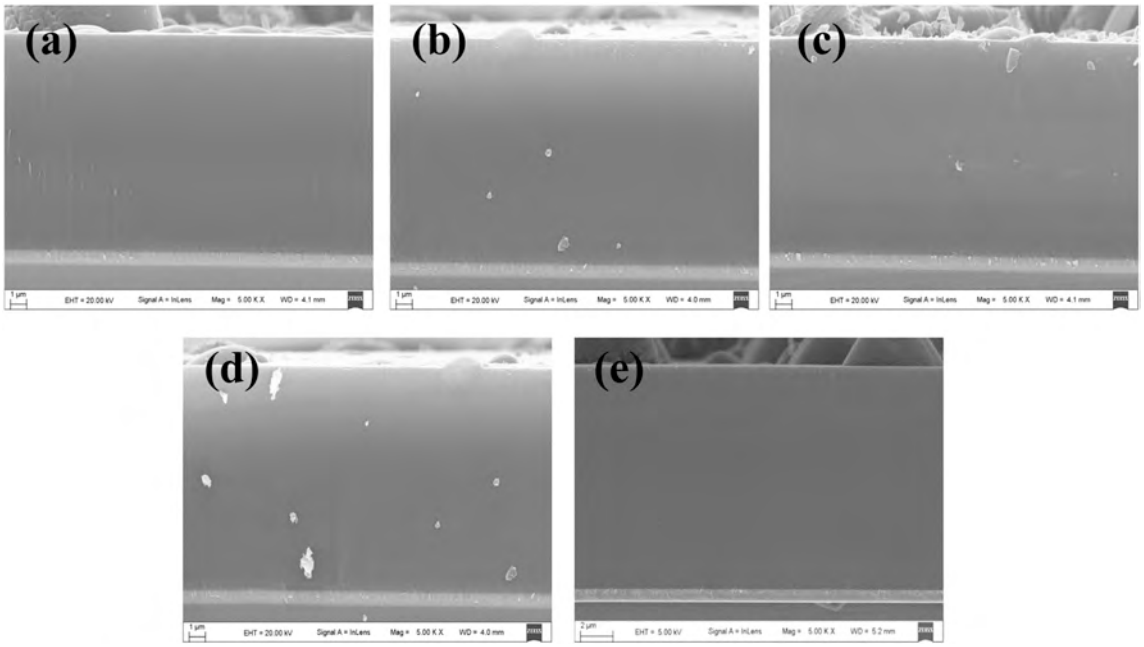

Fig. 2. SEM cross-sectional images of the DLC coatings deposited at (a) 1500 V (b) 3500 V (c) 5500 V (d) 7500 V (e) 9500 V pulsed biases.

deposited on Si (100) at pulsed biases of 1.5 kV, 3.5 kV, 5.5 kV, 7.5 kV, and 9.5 kV. The coatings have a similar thickness of about 13 μm including the 1.0 μm thick gradient Cr/CrCx/CrC interlayer [13]. The interfaces between the substrate, interlayer, and DLC coating show good adhesion due to energetic ion bombardment produced by HiPIMS discharge of the Cr target. A gradient morphology from columnar Cr to featureless C-rich CrC and gradient structure from crystalline to amorphous [13] can be observed from the interlayer. The DLC coatings do not have apparent defects regardless of pulsed bias.

Fig. 3 shows the Raman scattering and XPS results of the DLC coatings deposited on Si (100) at pulsed biases of 1.5 kV, 3.5 kV, 5.5 kV, 7.5 kV and 9.5 kV. Raman scattering is frequently used to characterize

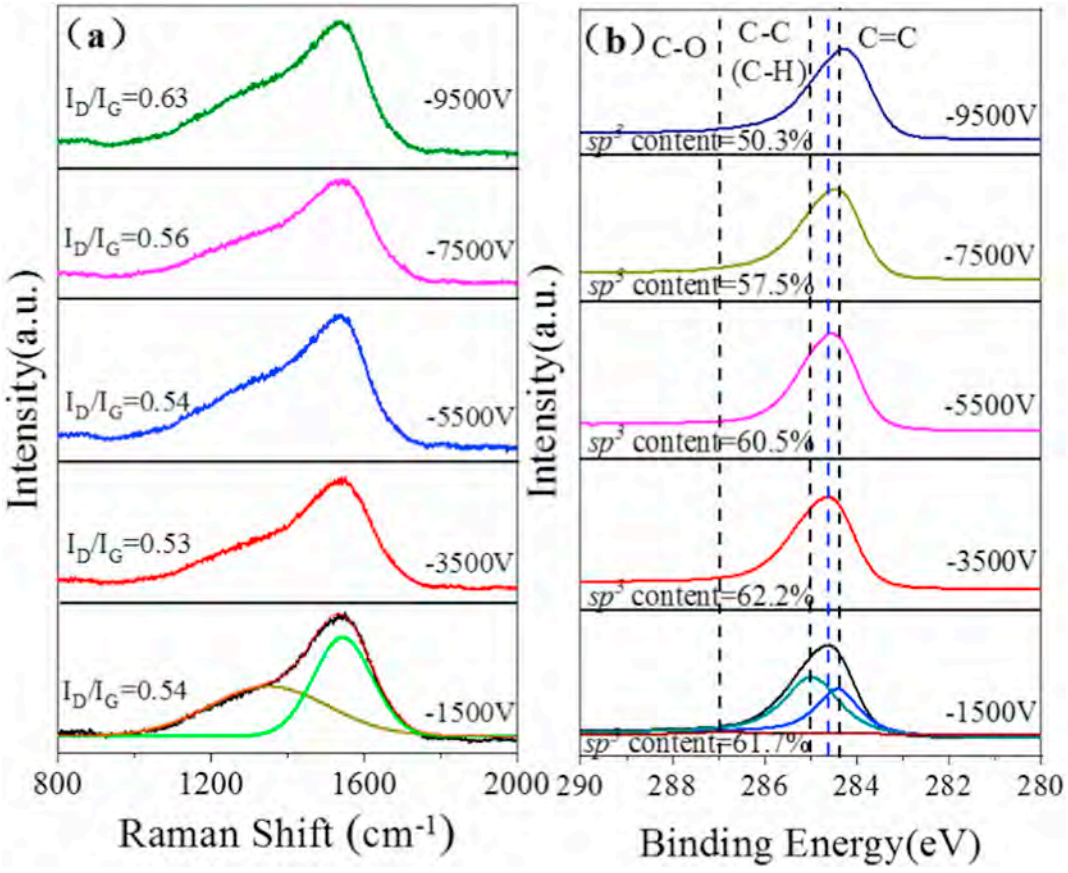

Fig. 3. (a) Raman scattering spectra and (b) XPS C1s spectra of prepared DLC coatings deposited at different pulsed bias.

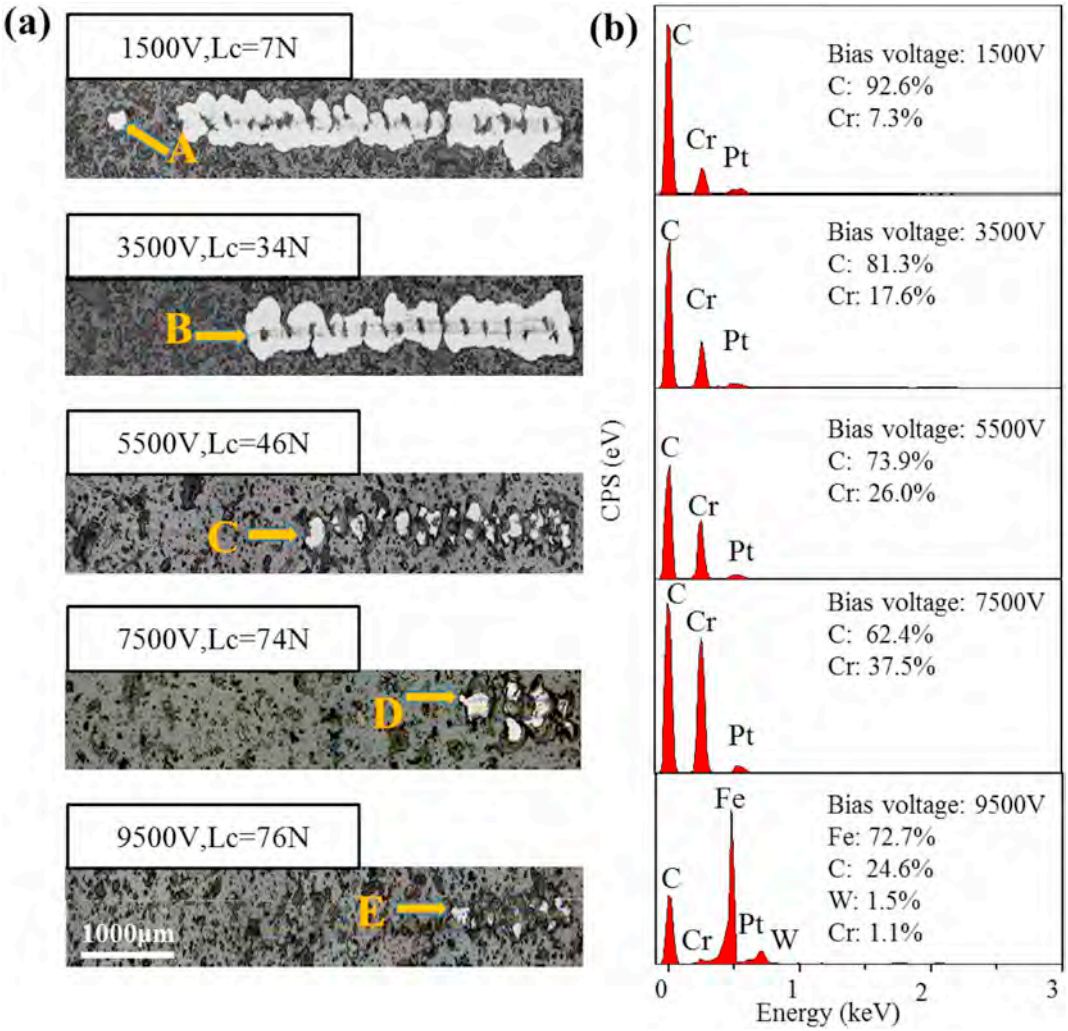

Fig. 4. (a) Scratch morphology and (b) EDS spectra showing the elemental composition of the DLC coatings deposited at different pulsed biases.

DLC coatings by determining the D peaks (at ~1345 cm^{-1}) and G peaks (at ~1580 cm^{-1}) using Gaussian fitting [5–7]. The G band represents the stretching mode of sp^2 carbon atoms in both rings and chains and the D band is related to the breathing mode of sp^2 in the rings [22–24]. Thus, the relative intensity ratio of the D peak (at 1348.87 cm^{-1}) to G peak (at 1543.41 cm^{-1}) (I_D/I_G) can indict the relative contents of sp^3 and sp^2 of DLC coatings [25]. Here, the I_D/I_G ratio is almost a constant at 0.54 when the pulsed bias is below 7.5 kV but increases to 0.63 if it is increased to 9.5 kV. Moreover, the position of G band is moving forward to high wavelength with the increasing of bias, suggesting that the transformation from sp^3 to sp^2 is affected by the heat generated by energetic ions [2]. The XPS C1s spectra in Fig. 3(b), which detected after 15 s etching by Ar ions, can be deconvoluted into two peaks using Gaussian fitting with bonding energies of 284.3 ± 0.1 eV and 285.2 ± 0.1 eV, corresponding to C=C sp^2 hybridized carbon atoms and C–C (together with C–H) sp^3 hybridized carbon atoms, respectively [11]. There is no obvious C–O peak can be calculated due to the surface etching by Ar ions. The shift of the C1 peak to a smaller binding energy is observed as the pulsed bias is increased. The sp^3 contents calculated from the peak areas, which are 61.7%, 62.2%, 60.5%, 57.5%, and 50.3% for pulsed biases of −1.5, −3.5 V, −5.5 V, −7.5 V, and −9.5 kV, respectively, indicating a relative large sp^3 content compared to those reported before [8], especially at a small pulsed bias.

As a result to the large internal stress, film delamination is a potential problem in practice. Scratch texts are performed to determine the adhesion strength of the DLC coatings on HSS deposited at 1.5 kV, 3.5 kV, 5.5 kV, 7.5 kV, and 9.5 kV and the scratch images are obtained by 3D laser scanning microscopy, as shown in Fig. 4(a). Both the locations of the semicircular cracks and the acoustic signals suggest delamination [26]. The data shows that the adhesion strength increases as the pulsed bias increased from 1.5 kV to 9.5 kV. The critical load (Lc) is improved significantly when the pulsed bias goes up from 1.5 kV to 9.5 kV and a large value of 76 N, which is few reported in previous published papers [27–29], is obtained from the DLC coating that is > 10 μm thick. To study the delamination characteristics, EDS is used to determine the compositions at points A-E after delamination as shown in Fig. 4(b). The major elements in the delaminated areas are Cr and C when the pulsed bias is below 7.5 kV, indicating that delamination occurs at the top interface between the interlayer and DLC coating. However, the Cr concentration increases while that of C decreases as the pulsed bias is increased, suggesting the delamination interface moves down to the Cr layer because of the gradient composition of the interlayer from Cr to C-rich CrC. When the pulsed bias is 9.5 kV, Fe, C, W are detected from point E, implying that delamination occurs at the interface between the HSS substrate and $Cr/CrC_x/CrC$ interlayer.

The excellent adhesion observed from the DLC coatings deposited at large pulsed biases can be attributed to two main factors. Firstly, a gradient $C/CrC_x/CrC$ interlayer is introduced to relax the mismatch [13,30] between the HSS substrate and DLC coating. The energetic Cr^+ produced by HiPIMS which offers high ionization of the sputtered materials [9] strengthens the interface between the HSS substrate and interlayer and consequently, delamination occurs at the top interface

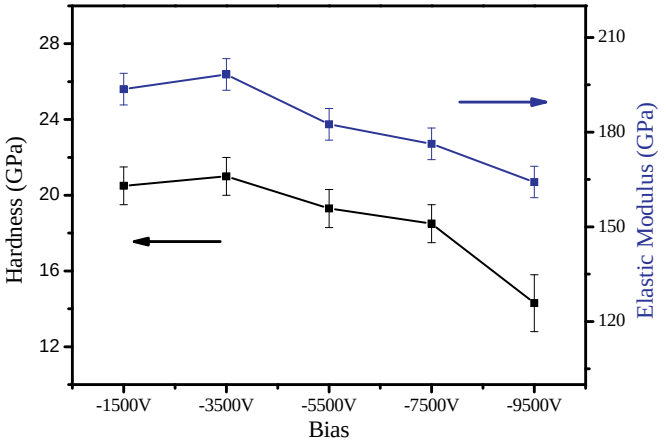

Fig. 5. Hardness and elastic modulus of the HSS substrate and DLC coatings deposited at different pulsed biases.

between the interlayer and DLC coating when the pulsed bias is < 7.5 kV. The energy of the highly ionized carbonous ions flux produced by the anode-layer ion source [33] increases with pulsed bias leading to a higher degree of ion implantation at the interface to enhance the adhesion strength between the interlayer and DLC coating [18]. When the pulsed bias is increased to 9.5 kV, adhesion at the top interface is better than that at the bottom interface between the substrate and the interlayer and so the delamination region moves down to the latter.

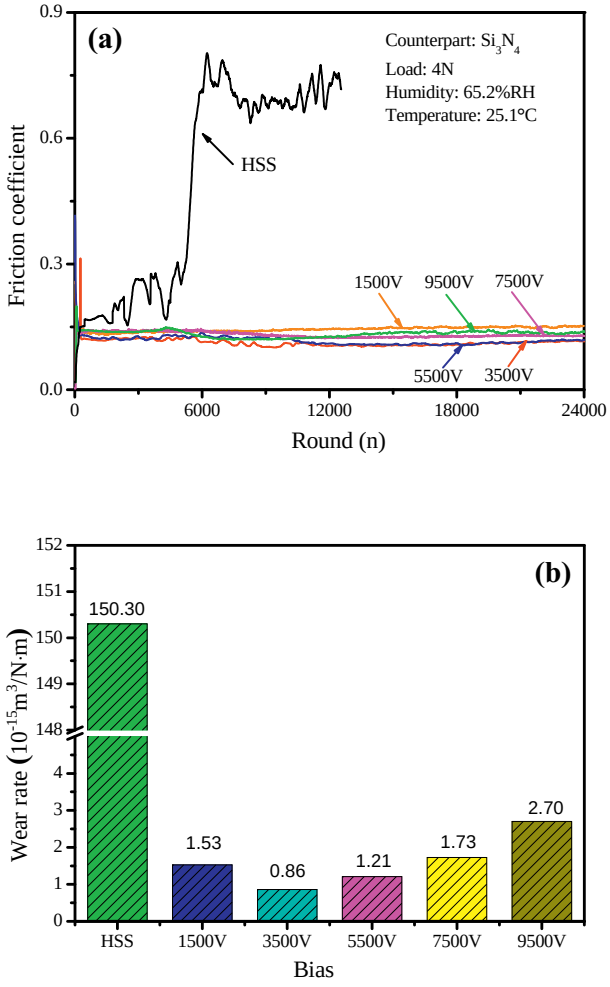

Fig. 6. (a) Friction coefficients and (b) Wear rates of the HSS substrate and DLC coatings deposited at different pulsed biases.

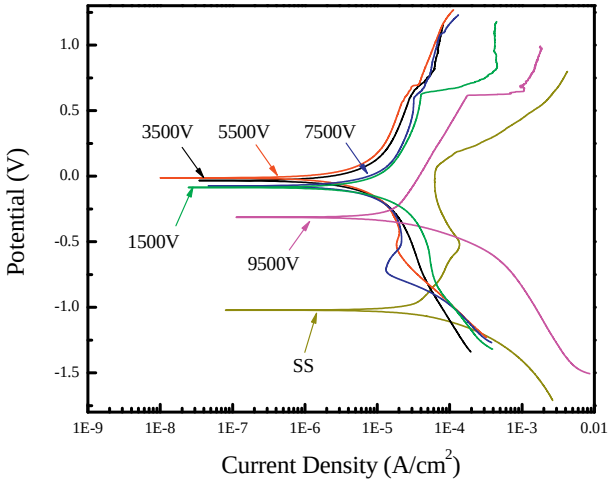

Fig. 7. Potentiodynamic test of the SS substrate and DLC coatings deposited at different pulsed biases.

The hardness and elastic modulus of the DLC coatings deposited on HSS at different pulsed biases are assessed by nano-indentation as shown in Fig. 5. The Dynamic Mechanical Analysis (DMA) mode adopted on the Hysitron TI 950 was used and the values presented here are averages of 5 measurements. The hardness and elastic modulus are similar when the pulsed bias is below 5.5 kV but decrease to 18.5 GPa and 176.3 GPa respectively, when the pulsed bias is increased to 7.5 kV. The obvious decrease occurs when the pulsed bias is 9.5 kV showing a hardness of 14.3 GPa, and it is related to the reduced sp^3 content [31–33], confirmed by XPS and Raman scattering (Fig. 3).

The tribological properties of the DLC coatings on HSS deposited at different pulsed biases are shown in Fig. 6(a) and (b). The friction coefficients exhibit a sharp drop in the beginning because of a transfer layer [34–36] on the surface and then stabilizes at 0.12–0.14 afterwards for the DLC coatings compared to about 0.7 on the HSS substrate. The wear rates of the DLC coatings show are consistent with that of the HSS substrate. The smallest friction coefficient of 0.12 and wear rate of 0.87×10^{-15} $m^3/N\,m$ is observed from the DLC coating deposited at 3.5 kV corresponding to the largest sp^3 content and hardness [37–39].

The electrochemical corrosion behaviors are investigated by potentiodynamic test. Fig. 7 shows the polarization curves of DLC coatings and SS substrate, and the details of corrosion current density and corrosion potential are listed in Table. 2. All DLC samples exhibit much better corrosion resistances than SS substrate which has the corrosion potential of −1.025 V and the corrosion current density of 45.9 μA/cm^2. When the pulsed bias is below 7500 V, no significant difference can be observed in the corrosion performance. Further increasing the pulsed bias, the decreased corrosion potential and increased corrosion current density occurs. The sample prepared with the pulsed bias of 5500 V shows the best corrosion properties with the largest corrosion potential of −17.2 mV and the smallest corrosion current density of 11.9 μA/cm^2, even compared with those prepared in the previous works

Table 2
The I_{corr} and E_{corr} results of SS and DLC coatings deposited at different pulsed biases.

Sample	E_{corr}/mV	I_{corr}/μA·cm^{-2}
SS	−1025	45.9
1500 V	−88.0	21.5
3500 V	−35.2	18.6
5500 V	−17.2	11.9
7500 V	−77.2	18.8
9500 V	−314.6	29.1

[40–42]. All the features are consistent with the evolution of the sp^3 content and the hardness [43–45], suggesting the important effect of the hybridization ratio (sp^3/sp^2) in the DLC induced by the excess ion bombardment [46].

4. Conclusion

To enhance the adhesion between a thick DLC coating and HSS substrate and simultaneously avoid graphitization at a high temperature, pulsed kV biases are applied to deposit the DLC coatings. The intermittent energetic ion bombardment and implantation enhances not only the adhesion between the 13 μm thick DLC coating to > 70 N, but also the sp^3 content and mechanical and electrochemical corrosion behaviors including the hardness, wear resistance and corrosion resistance. Our results suggest an effective strategy to fabricate thick DLC coatings with good adhesion, strength mechanical properties and excellent corrosion behaviors.

Acknowledgements

This work was jointly financially supported by National Materials Genome Project (No. 2016YFB0700600), Shenzhen Science and Technology Innovation Commission Research Grants (JCYJ20150828093127698 and JCYJ20170306165240649), and City University of Hong Kong Applied Research Grant (ARG) No. 9667122.

References

[1] A. Anders, I.G. Brown, K.M. Yu, Increase the retained dose by plasma immersion ion implantation and deposition, Beam Interact. Mater. Atoms 12 (1995) 132–135.
[2] J.D. Drescher, H.J. Scheibe, A. Mensch, A model for particle growth in arc deposited amorphous carbon films, Diam. Relat. Mater. 7 (1998) 1375–1380.
[3] H. Mohrbacher, J.P. Celis, Friction mechanisms in hydrogenated amorphous carbon coatings, Diam. Relat. Mater. 4 (1995) 1267–1270.
[4] A. Grill, Diamond-like carbon coatings as biocompatible materials-an overview, Diam. Relat. Mater. 12 (2003) 166–170.
[5] A. Grill, Diamond-like carbon state of the art, Diam. Relat. Mater. 8 (1999) 428–434.
[6] A. Gangopadhyay, K. Sinha, D. Uy, D.G. McWatt, R.J. Zdrodowski, S.J. Simko, Friction, Wear, and surface film formation characteristics of diamond-like carbon thin coating in valvetrain application, Tribol. Trans. 54 (2010) 104–114.
[7] F. Cemin, C.D. Boeira, C.A. Figueroa, On the understanding of the silicon-containing adhesion interlayer in DLC deposited on steel, Tribol. Int. 94 (2016) 464–469.
[8] J. Robertson, Diamond-like amorphous carbon, Mater. Sci. Eng. R 37 (2002) 129–281.
[9] C.W. Zou, H.J. Wang, L. Feng, S.W. Xue, Effects of Cr concentrations on the microstructure, hardness, and temperature-dependent tribological properties of Cr-DLC coatings, Appl. Surf. Sci. 286 (2013) 137–141.
[10] A.-Y. Wang, H.-S. Ahn, K.-R. Lee, J.-P. Ahn, Unusual stress behavior in W-incorporated hydrogenated amorphous carbon films, Appl. Phys. Lett. 86 (2005) 111902.
[11] T. Topalovic, V.A. Nierstrasz, L. Bautista, D. Jocic, A. Navarro, M.M.C.G. Warmoeskerken, XPS and contact angle study of cotton surface oxidation by catalytic bleaching, Colloids Surf. A Physicochem. Eng. Asp. 296 (2007) 76–85.
[12] P.H. Gaskell, A. Saeed, P.C. Chieux, D.R. McKenzie, Neutron-scattering studies of the structure of highly tetrahedral amorphous diamond like carbon, Phys. Rev. Lett. 67 (1988) 1286.
[13] L. Liu, Z. Wu, X. An, S. Xiao, S. Cui, H. Lin, R.K.Y. Fu, X. Tian, R. Wei, P.K. Chu, F. Pan, Excellent adhered thick diamond-like carbon coatings by optimizing hetero-interfaces with sequential highly energetic Cr and C ion treatment, J. Alloys Compd. 735 (2018) 155–162.
[14] B. Tang, H. Liu, L. Wang, X. Wang, K. Gan, Y. Yu, Y. Wang, T. Sun, S. Wang, Fabrication of titanium carbide film on bearing steel by plasma immersion ion implantation and deposition, Surf. Coat. Technol. 186 (2004) 320–323.
[15] J. Sui, W. Cai, L. Zhao, Surface modification of NiTi alloys using diamond-like carbon (DLC) fabricated by plasma immersion ion implantation and deposition (PIIID), Nucl. Instrum. Methods Phys. Res., Sect. B 248 (2006) 67–70.
[16] Z. Xu, H. Sun, Y.X. Leng, X. Li, W. Yang, N. Huang, Effect of modulation periods on the microstructure and mechanical properties of DLC/TiC multilayer films deposited by filtered cathodic vacuum arc method, Appl. Surf. Sci. 328 (2015) 319–324.
[17] Y. Lifshitz, G.D. Lempert, E. Grossman, I. Avigal, C. Uzan-Saguy, R. Kalish, J. Kulik, D. Marton, J.W. Rabalais, Growth mechanisms of DLC films from C+ ions: experimental studies, Diam. Relat. Mater. 4 (1995) 318–323.
[18] J. Wang, W.-Z. Li, H.-D. Li, Influence of the bombardment energy of CH^{n+} ions on the properties of diamond-like carbon films, Surf. Coat. Technol. 122 (1999) 273–276.
[19] G. Li, C. Liu, J. Li, C. Zhang, Z. Mu, Z. Long, Plasma-ion beam source enhanced deposition system, Surf. Coat. Technol. 193 (2005) 112–116.
[20] S. Bhowmick, M.Z.U. Khan, A. Banerji, M.J. Lukitsch, A.T. Alpas, Low friction and wear behaviour of non-hydrogenated DLC (a-C) sliding against fluorinated tetrahedral amorphous carbon (ta-C-F) at elevated temperatures, Appl. Surf. Sci. 450 (2018) 274–283.
[21] N. Ren, Z.J. Ma, D.C. Zhao, G.J. Xiao, S.H. Wu, Preparation and property of a Fe-doped DLC multilayer by ion sources, Mater. Sci. Forum 654-656 (2010) 1908–1911.
[22] Z. Xu, Y.J. Zheng, F. Jiang, Y.X. Leng, H. Sun, N. Huang, The microstructure and mechanical properties of multilayer diamond-like carbon films with different modulation ratios, Appl. Surf. Sci. 264 (2013) 207–212.
[23] J.-B. Wu, J.-J. Chang, M.-Y. Li, M.-S. Leu, A.-K. Li, Characterization of diamond-like carbon coatings prepared by pulsed bias cathodic vacuum arc deposition, Thin Solid Films 516 (2007) 243–247.
[24] Y. Wang, Y. Ye, H. Li, L. Ji, Y. Wang, X. Liu, J. Chen, H. Zhou, Microstructure and tribological properties of the a-C:H films deposited by magnetron sputtering with CH4/Ar mixture, Surf. Coat. Technol. 205 (2011) 4577–4581.
[25] T. Takeno, T. Komiyama, H. Miki, T. Takagi, T. Aoyama, XPS and TEM study of W-DLC/DLC double-layered film, Thin Solid Films 517 (2009) 5010–5013.
[26] G.F. Yina, C.Q. Zhenga, H.H. Tongb, Y.F. Huob, L.L. Mu, Preparation of DLC gradient biomaterials by means of plasma source ion implant-ion beam enhanced deposition, Thin Solid Films 245 (1999) 67–70.
[27] K.-R. Lee, K. Yong Eun, I. Kim, J. Kim, Design of W buffer layer for adhesion improvement of DLC films on tool steels, Thin Solid Films 377-378 (2000) 261–268.
[28] M. Yatsuzuka, Y. Oka, M. Nishijima, K. Hiraga, Microstructure of interface for high-adhesion DLC film on metal substrates by plasma-based ion implantation, Vacuum 83 (2008) 190–197.
[29] D. Bootkul, B. Supsermpol, N. Saenphinit, C. Aramwit, S. Intarasiri, Nitrogen doping for adhesion improvement of DLC film deposited on Si substrate by filtered cathodic vacuum arc (FCVA) technique, Appl. Surf. Sci. 310 (2014) 284–292.
[30] Z. Yang, J. Lian, J. Wang, Molecular dynamics simulation of thin film interfacial strength dependency on lattice mismatch, Thin Solid Films 537 (2013) 190–197.
[31] L. Xia, M. Sun, J. Liao, The effect of negative bias pulse on the bonding configurations and properties of DLC films prepared by PBII with acetylene, Diam. Relat. Mater. 14 (2005) 42–47.
[32] A. Ferrec, J. Keraudy, S. Jacq, F. Schuster, P.Y. Jouan, M.A. Djouadi, Correlation between mass-spectrometer measurements and thin film characteristics using dcMS and HiPIMS discharges, Surf. Coat. Technol. 250 (2014) 52–56.
[33] P. Ye, F. Xu, J. Wu, S. Tian, X. Zhao, X. Tang, D. Zuo, Effects of anode layer linear ion source on the microstructure and mechanical properties of amorphous carbon nitride films, Surf. Coat. Technol. 320 (2017) 183–189.
[34] H. Liu, Q. Xu, C. Wang, X. Zhang, B. Tang, Investigating the microstructure and mechanical behaviors of DLC films on AISI52100 bearing steel surface fabricated by plasma immersion ion implantation and deposition, Surf. Coat. Technol. 228 (2013) S159–S163.
[35] Y. Liu, Tribological behavior of DLC coatings with functionally gradient interfaces, Surf. Coat. Technol. 153 (2002) 178–183.
[36] J.D. Schall, G. Gao, J.A. Harrison, Effects of adhesion and transfer film formation on the tribology of self-mated DLC contacts, J. Phys. Chem. C 114 (2010) 5321–5330.
[37] K. Yamamoto, K. Matsukado, Effect of hydrogenated DLC coating hardness on the tribological properties under water lubrication, Tribol. Int. 39 (2006) 1609–1614.
[38] M. Lubwama, B. Corcoran, K. Sayers, J.B. Kirabira, A. Sebbit, K.A. McDonnell, D. Dowling, Adhesion and composite micro-hardness of DLC and Si-DLC films deposited on nitrile rubber, Surf. Coat. Technol. 206 (2012) 4881–4886.
[39] B.C. Na, A. Tanaka, Tribological characteristics of diamond-like carbon films based on hardness of mating materials, Thin Solid Films 478 (2005) 176–182.
[40] R. Hatada, S. Flege, A. Bobrich, W. Ensinger, K. Baba, Surface modification and corrosion properties of implanted and DLC coated stainless steel by plasma based ion implantation and deposition, Surf. Coat. Technol. 256 (2014) 23–29.
[41] G. Wu, W. Dai, H. Zheng, A. Wang, Improving wear resistance and corrosion resistance of AZ31 magnesium alloy by DLC/AlN/Al coating, Surf. Coat. Technol. 205 (2010) 2067–2073.
[42] S. Bhattacherjee, H. Niakan, Q. Yang, Y. Hu, J. Dynes, Enhancement of adhesion and corrosion resistance of diamond-like carbon thin films on Ti–6Al–4V alloy by nitrogen doping and incorporation of nanodiamond particles, Surf. Coat. Technol. 284 (2015) 153–158.
[43] J.C. Damasceno, S.S. Camargo, F.L. Freire, R. Carius, Deposition of Si-DLC films with high hardness, low stress and high deposition rates, Surf. Coat. Technol. 133-134 (2000) 247–252.
[44] Y. Mabuchi, T. Higuchi, V. Weihnacht, Effect of sp^2/sp^3 bonding ratio and nitrogen content on friction properties of hydrogen-free DLC coatings, Tribol. Int. 62 (2013) 130–140.
[45] S. Zhang, Y. Fu, H. Du, X.T. Zeng, Y.C. Liu, Magnetron sputtering of nanocomposite (Ti,Cr)CN/DLC coatings, Surf. Coat. Technol. 162 (2003) 42–48.
[46] Z. Wang, C.B. Wang, Q. Wang, J.Y. Zhang, Electrochemical corrosion behaviors of a-C:H and a-C:N_X:H films, Appl. Surf. Sci. 254 (2008) 3021–3025.